Neutral Current Minimization Control for Solid State Transformers under Unbalanced Loads in Distribution Systems

Junru Chen, *Student Member, IEEE,* Tao Yang, Cathal O'Loughlin and Terence O'Donnell, *Member, IEEE*

***Abstract*—This paper analyses the neutral current reduction performance of a three phase four leg solid state transformer (SST) under different degrees of unbalanced load. Several kinds of control strategies are presented, the neutral current elimination controls which rely on phase shifting, voltage amplitude and phase shifting & voltage amplitude combination control. A neutral current minimization control which ensures the SST output voltages complies with the EN 50160 output voltage unbalance standard is also developed. These control approaches simply build on the balanced voltage control providing voltage references which slightly unbalanced the voltage amplitude and phase angle or both. The effectiveness of the proposed strategies is validated through tests on a downscaled prototype. Simulation results for the neutral current minimization control of the SST applied to a real urban distribution network with distributed loads are presented. The results of this analysis show that overall the neutral current minimization results in an energy saving from both reduced losses in the distribution cables and reduced power consumption in the load.**

***Index Terms*—Neutral Current, Solid State Transformer, Smart Transformer, Unbalanced Loads, Distribution Systems.**

I. Introduction

Improvements in the performance of power electronics devices coupled with the move towards a smarter more controllable grid has motivated interest in the development of the Solid State Transformer (SST) for applications in the distribution system [1][2]. Unlike the conventional line frequency transformer, the SST is an active controllable device which offers the potential for input-output decoupling, active voltage regulation and power flow control. The SST has been proposed as an important element in managing the incorporation of distributed energy resources (DER) [3][4] and storage systems [5][6]. However to date full scale prototype SSTs have only achieved efficiencies in the range of 96.75% [7][8]. Clearly this is less than the typical quoted efficiency for a line frequency distribution transformer (LFT) which is in the range of 98%-99.5%. To compensate the losses, the ancillary services to enhance grid operation which can be provided by the SST, is emphasized in the concept of the smart transformer (ST) [9]. Among the ancillary services investigated in recent literature is the ability to provide on-demand reactive power support for the MV grid [10], power management [11][12] and stability [13] in microgrids [14], maintenance of the stability of the LV grid in the presence of increasing penetration of DER [15][16], online load identification [17] and control of distribution system power generation [18][19] and consumption [20]. Following in this research vein of investigating the system level benefits of the controllable ST, this work investigates the application of an ST to the reduction of neutral currents which arise due to unbalanced loading in the distribution network.

Unbalanced loading is quite common in the modern distribution grid with the growth of dynamically varying domestic loads. Such unbalance may well increase in the future with the introduction of new loads such as electric vehicle charging points [21]. The problems associated with unbalanced loads in the distribution system have been discussed previously in the literature by Jouanne et al. [22]. For example in a 4-wire distribution systems, the unbalance loads can cause excessive current in the neutral wire, thus giving rise to voltage drop along the neutral wire resulting in ground voltage fluctuation for customers [23][24]. Furthermore, excessive neutral current could produce increased losses in the neutral wire. However, it is possible that an SST implementing an appropriate control function, could reduce or eliminate this excessive neutral current by regulating its output voltage. For example, in the context of unbalanced loads in data centers, reference [25] and [26] described a concept and provided three different control methods to eliminate the neutral current by the means of dynamically adjusting the relative amplitudes and the mutual phase differences of the three phase voltages respectively. However, in a distribution system context, the allowable degree of unbalance in the utility supply voltages must adhere

Manuscript received July, 03, 2018; revised September, 21, 2018, accepted November, 11, 2018. This work has supported in part by the Science Foundation Ireland (SFI) Strategic Partnership Programme Grant Number SFI/15/SPP/E3125.

Junru Chen, Cathal O'Loughlin and Terence O'Donnell are with the Energy Institute, University College Dublin, Dublin, Ireland. (e-mail: junru.chen.1@ucdconnect.ie;oloughlin.cathal@ucd.ie;Terence.odonnell@ucd.ie)

Tao Yang is with the WANMA Group, Xihu Distinct, Hangzhou, Zhejiang, China. (e-mail:tao.yang@ucdconnect.ie)

to standards such as EN 50160 [27], so that a wide variation in relative voltage amplitude and phase between phases is not allowable. The contribution of this work is in the development of a neutral current minimization control strategy for the SST which meets the requirement of voltage supply standards- EN 50160 [27] and is also shown to have the potential for energy saving from the aspect of the whole distribution system. The energy saving possible when the method is applied to an example urban distribution system with a typical unbalanced load profile is investigated.

The paper is structured as follows: Section II briefly reviews the solid state transformer in the distribution system. Section III reviews the neutral current elimination control strategy for the three phase four wire SST under unbalanced loads. Section IV introduces the proposed neutral current minimization control which ensures adherence to the requirements for voltage unbalance in the distribution system. Section V presents hardware validation of the control method on a 220 V 4 kVA downscaled prototype of a 3-phase 4-leg inverter. Finally, section VI provides simulation results for the implementation of the control approach in an actual distribution network with distributed loads and assesses the energy savings possible while Section VII draws the conclusions.

II. SST Configuration

Similar to the traditional transformer, the SST provides a step-up or step-down voltage function, but with advanced functionality. In this work we use a three phase version of the three stage SST found to be one of the most suitable in terms of input/output decoupling by Falcones et al. [28]. Fig.1. shows the basic configuration of the 3-stage SST consisting of an AC/DC rectifier, Dual Active Bridge (DAB) DC-DC converter with a high frequency transformer and a DC/AC inverter. The rectifier converts the medium voltage grid frequency three-phase AC input voltage into a medium voltage DC. The next step consists of a Dual Active Bridge (DAB) that transforms the medium DC voltage using a high frequency transformer, to a low voltage DC output. Finally, an inverter at the output stage converts the low DC voltage to a power frequency three-phase AC voltage connected to the load.

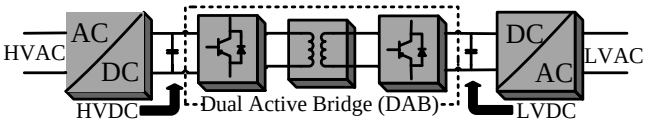

Fig.1. Basic configuration of three-stage SST.

The low voltage inverter output stage consists of a three phase, 4-leg inverter, allowing connection to a four wire LV distribution system, with the fourth leg connected to the neutral wire. The SST topology is shown in Fig. 2. By application of the three-dimensional space vector modulation (3-D SVPWM), each phase can be independently regulated through the fourth leg, thus control of the three phase voltages are decoupled [29][30].

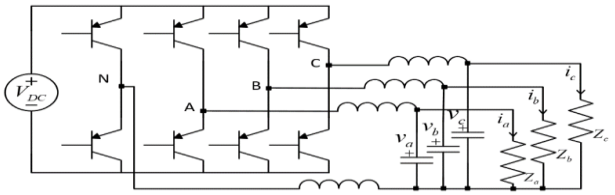

Fig. 2. Overall three-Phase four-leg SST topology.

III. Neutral Current Elimination Control

In order to illustrate the approach to neutral current elimination or minimization, consider that the distribution system supplied by the SST can be simplified to be represented by three single phase constant impedance loads, Z_a, Z_b and Z_c as shown in Fig. 2.

Assuming that the SST output voltages are given by the balanced three phase supplies:

$$v_a = V_a\cos(\omega t), v_b = V_b\cos\left(\omega t - \tfrac{2\pi}{3}\right), v_c = V_c\cos\left(\omega t + \tfrac{2\pi}{3}\right) \quad (1)$$

Then the corresponding phase currents will be:

$$\left.\begin{aligned} i_a &= I_a\cos(\omega t - \theta_{za}) \\ i_b &= I_b\cos\left(\omega t - \frac{2\pi}{3} - \theta_{zb}\right) \\ i_c &= I_c\cos\left(\omega t + \frac{2\pi}{3} - \theta_{zc}\right) \end{aligned}\right\} \quad (2)$$

Where $\theta_{za}, \theta_{zb}, \theta_{zc}$ are the load angles of the phases, a, b and c and the phase currents are generally unbalanced.

The unbalanced phase currents could be balanced by adjusting the voltage phase angles, amplitudes or both. Consider that we can control the angles and amplitudes of two of the SST output phase voltages relative to the other as follows:

$$\left.\begin{aligned} v_a &= V_a\cos(\omega t) \\ v_b &= \rho_b V_a\cos\left(\omega t - \frac{2\pi}{3} + \gamma_b\right) \\ v_c &= \rho_c V_a\cos(\omega t + \frac{2\pi}{3} + \gamma_c) \end{aligned}\right\} \quad (3)$$

Where ρ_b, ρ_c scale the amplitude of phase b and c respectively relative to phase a, and γ_b, γ_c introduce an extra phase shift in phase b and c respectively thus introducing an unbalance in the voltage. Previous works [25][26] have shown that the phase currents can be balanced by the use of the phase shift angles γ_b, γ_c alone (with $\rho_b = \rho_c = 1$), by use of the amplitude scaling factors, ρ_b, ρ_c alone (with $\gamma_a = \gamma_b = 0$) or by a combination of both phase shift and amplitude scaling. For example, in [25] it was shown that using phase shifting alone, if the angles of the phase currents $(\theta_a, \theta_b, \theta_c)$ are set as:

$$\left.\begin{aligned} \theta_a &= -\theta_{za} \\ \theta_b &= arccos\left(-\frac{I_c^2 - I_a^2 - I_b^2}{2I_aI_b}\right) - \pi - \theta_{zb} \\ \theta_c &= arccos\frac{I_b^2 - I_a^2 - I_c^2}{2I_aI_c} - \theta_{zc} \end{aligned}\right\} \quad (4)$$

Then the resulting currents are balanced and the neutral current is eliminated. This implies that the required phase shift for the voltages would be:

$$\gamma_{b0} = \theta_b + \theta_{zb} + \frac{2\pi}{3}, \quad \gamma_{c0} = \theta_c + \theta_{zc} - \frac{2\pi}{3} \quad (5)$$

Note that this is subject to the constraint that

$$\left|\frac{I_c^2 - I_a^2 - I_b^2}{2I_aI_b}\right| < 1, \left|\frac{I_b^2 - I_a^2 - I_c^2}{2I_aI_c}\right| < 1 \quad (6)$$

Which means $I_a \le I_b + I_c$, $I_b \le I_a + I_c$, $I_c \le I_b + I_a$, i.e. no phase current amplitude should be greater than the sum of the other two.

Alternatively, making use of amplitude scaling alone (i.e. $\gamma_b = \gamma_c = 0$), then the neutral current can be eliminated by using the amplitude scaling factors:

$$\rho_b = \frac{sin(\theta_a - \theta_c)}{sin(\theta_c - \theta_b)} * \frac{|Z_b|}{|Z_a|}, \rho_c = \frac{sin(\theta_a - \theta_b)}{sin(\theta_b - \theta_c)} * \frac{|Z_c|}{|Z_a|} \quad (7)$$

Note that in general the reference phase can be taken as any of the phases and in the case of amplitude scaling it may be more appropriate to choose the reference phase as the phase with the minimum amplitude current. However, for ease of notation here we have assumed that this is phase a.

The neutral current could also be eliminated by combining both phase shifting and amplitude scaling. Using this approach the concept is that voltage amplitude control determines the amplitudes of the resulting currents which meet the necessary constraints for phase shift control in (6). After the amplitude of the reference voltage is selected and consequently the amplitude of the phase current is determined, and then the phase angle can be calculated by phase shift control to eliminate the neutral current. The full details of voltage references calculation for the three control strategies can be found in [25] and [26].

IV. Neutral Current Minimization Control

The problem with the methods above for application in a distribution system is that standards [27] place limits on the allowable voltage unbalance. For example, the EN 50160 [27] standard which applies to the voltage characteristics in public distribution systems specifies that the unbalanced voltage degree in the distribution system should be below 2% for 95% of the time, with the voltage unbalance defined as the ratio of the negative sequence to the positive sequence component [27]. The estimation of this voltage unbalance degree can be obtained according to (8) and (9) [31].

$$\mathrm{PVUR} = \frac{V_{max} - V_{min}}{V_{avg}} \times 100\% \quad (8)$$

$$\mathrm{UBF} = \left|\frac{V_n}{V_p}\right| \times 100\% \quad (9)$$

Where, $V_{max}/V_{min}/V_{avg}$ is the maximum/minimum/average value of the amplitude of output voltage and V_n/V_p is the negative/positive sequence of output voltage.

The maximum allowable value is 2% for both of these measures of unbalance. This makes it unlikely, especially for larger load unbalances, that the calculations in (8) and (9) give phase angles and amplitudes which are within the allowable range of unbalance. Hence in this case the neutral current cannot be completely eliminated. However, applying a combination of phase shifting and amplitude control on the SST output voltage, which still adheres to these limits still, has the potential to reduce and minimize the neutral current.

A. Neutral Current Minimization with Constraints

The amplitude unbalance degree limitation restricts the voltage amplitude, and phase unbalance degree limitation mainly restricts the phase shifting angle of the voltage. Therefore, the approach to reduce neutral current proceeds in two steps, first the output voltage amplitude references are obtained, and subsequently the phase angle references obtained. In the first step the amplitudes of the voltages are regulated to make the amplitudes of the resulting currents meet the constraints required for phase shift control as outlined in (6) and the amplitudes of the voltages are also regulated for the minimization of neutral current within the amplitude unbalance limitation. As long as the phase currents meet the constraints for phase shift control, the zero neutral current solution could be obtained by the phase shift control as in (5). However, as the reference phase angles obtained from this solution for zero neutral current may violate the phase unbalance constraints, it is necessary to calculate phase shift angles, γ_b, γ_c which minimize the neutral current but still satisfy the constraint in (9).

B. Voltage Amplitude Reference Calculation

Making use of voltage scaling factors then the amplitudes of the resulting currents can be written as:

$$I_a = \frac{V_a}{|Z_a|}; \; I_{bm} = \frac{\rho_b V_a}{|Z_b|}; \; I_c = \frac{\rho_c V_a}{|Z_c|} \quad (10)$$

There are several conditions which the choice of the relative amplitude factors must satisfy. According to (6) in order to ensure that a solution exists for zero neutral current under phase shift control, the relative amplitude correction factors ρ_b, ρ_c need to be chosen in the following range:

$$\frac{1}{Z_a} \le \frac{\rho_b}{Z_b} + \frac{\rho_c}{Z_c}, \quad \frac{\rho_b}{Z_b} \le \frac{1}{Z_a} + \frac{\rho_c}{Z_c}, \quad \frac{\rho_c}{Z_c} \le \frac{1}{Z_a} + \frac{\rho_b}{Z_b} \quad (11)$$

In addition if V_{min}, and V_{max} are the minimum and maximum allowable amplitude values of the output phase voltages for the system then it should be ensured that the voltages do not fall outside this range, i.e. :

$$\left.\begin{array}{l} \min(V_{ma}, \rho_b V_{ma}, \rho_c V_{ma}) > V_{min} \\ \max(V_{ma}, \rho_b V_{ma}, \rho_c V_{ma}) < V_{max} \end{array}\right\} \quad (12)$$

The voltage amplitude unbalanced constraint of (8), can be rewritten in terms of the factors, ρ_b, ρ_c as:

$$\frac{\max(1, \rho_b, \rho_c) - \min(1, \rho_b, \rho_c)}{(1 + \rho_b + \rho_c)/3} \le 2\% \quad (13)$$

The scaling factors are chosen as the maximum allowable which still satisfy (13). According to [20][32], the load is positively dependent on voltage. Thus, voltage reduction could help to reduce the current or demand. Here we set the scaling factor of the phase with largest load to the minimum value of 0.98, and of the phase with smallest load to the reference phase a. The remaining phase voltage is set to 0.99.

C. Phase Shifting Reference Calculation

Now consider the relationship between the voltage phase

unbalance constraint in (9) which is constrained to be less than 2% and the relative phase shift angles. The voltage phase unbalance constraint, the positive and negative sequence voltage components and the voltage amplitude unbalance constraint can be represented by the following equations:

$$\mathrm{UBF} = \left|\frac{\mathrm{V_n}}{\mathrm{V_p}}\right| \times 100\% \leq 2\% \tag{14}$$

$$\mathrm{V_n} = \mathrm{V_{ma}}\angle 0 + \mathrm{V_{mb}}\angle\left(-120 + \gamma_{\mathrm{b}}\right) * 1\angle -120 + \mathrm{V_{mc}}\angle\left(120 + \gamma_{\mathrm{c}}\right) * 1\angle 120 \tag{15}$$

$$\mathrm{V_p} = \mathrm{V_{ma}}\angle 0 + \mathrm{V_{mb}}\angle\left(-120 + \gamma_{\mathrm{b}}\right) * 1\angle 120 + \mathrm{V_{mc}}\angle\left(120 + \gamma_{\mathrm{c}}\right) * 1 - 120 \tag{16}$$

$$0.98 * \max(\mathrm{V_{ma}}, \mathrm{V_{mb}}, \mathrm{V_{mc}}) \leq \min(\mathrm{V_{ma}}, \mathrm{V_{mb}}, \mathrm{V_{mc}}) \tag{17}$$

We want to use the voltage phase unbalance constraint to determine the limitation for phase shifting angle γ_{b} and γ_{c}. By expanding (15) and (16) and making the assumption that sin(γ) = 0 for small γ, the voltage unbalance in (14) can be written as (18), which is valid for small values of γ_b and γ_c:

$$\frac{|\mathrm{V_n}|^2}{|\mathrm{V_p}|^2} = \frac{1 + \rho_{\mathrm{b}}^2 + \rho_{\mathrm{c}}^2 - \rho_{\mathrm{b}}\cos(\gamma_{\mathrm{b}}) - \rho_{\mathrm{c}}\cos(\gamma_{\mathrm{c}}) - \rho_{\mathrm{b}}\rho_{\mathrm{c}}\cos(\gamma_{\mathrm{b}} + \gamma_{\mathrm{c}})}{(1 + \rho_{\mathrm{b}} + \rho_{\mathrm{c}})^2} \tag{18}$$

Making use of (18) Fig. 3 plots the UBF for of γ_b and γ_c in the range of +/- 5 degrees and for amplitude scaling factors, $\rho_b = \rho_c = 1$. Also plotted is the plane representing the 2% limitation on UBF.

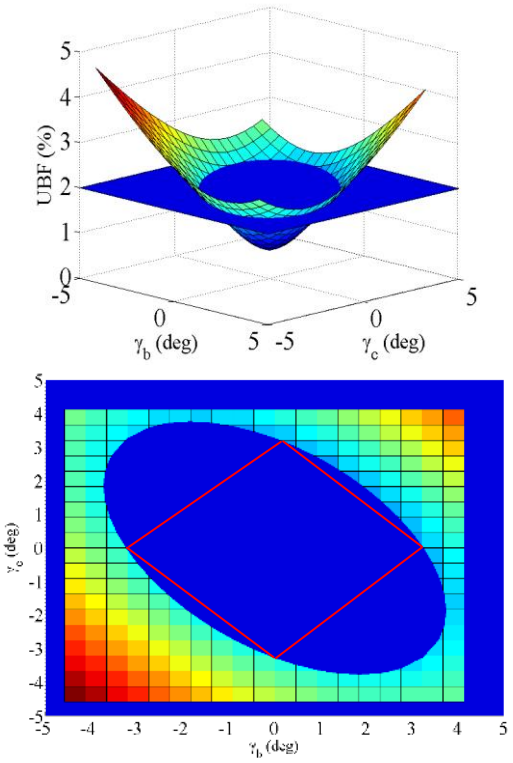

Fig. 3. UBF, vs. $\gamma_{b,}\gamma_c$ with 2% unbalance constraint.

The intersection of the UBF and the 2% limit form an elliptical boundary for γ_b and γ_c, and for any combination of γ_b and γ_c which falls inside this boundary the UBF constraint is satisfied. Indeed if the cosine terms in (18) are approximated by the first two terms of a Taylor series expansion, then this quadratic relationship becomes clearer and it can be shown that in general (18) can be written in the form:

$$a\gamma_b^2 + b\gamma_c^2 + c\gamma_b\gamma_c + d \tag{19}$$

Where:

$$a = \frac{(\rho_b+\rho_b\rho_c)}{2(1+\rho_b+\rho_c)^2},\ b = \frac{(\rho_c+\rho_b\rho_c)}{2(1+\rho_b+\rho_c)^2},\ c = \frac{\rho_b\rho_c}{(1+\rho_b+\rho_c)^2},$$

$$d = \frac{1+\rho_b^2+\rho_c^2-\rho_b-\rho_c-\rho_b\rho_c}{(1+\rho_b+\rho_c)^2}$$

For the constraint to be satisfied, γ_b and γ_c must satisfy the following relationship:

$$a\gamma_b^2 + b\gamma_c^2 + c\gamma_b\gamma_c + d \leq (0.02)^2 \tag{20}$$

If the relationship between γ_b and γ_c and the magnitude of neutral current were now known then (20) could be used to find the optimum combination of γ_b and γ_c which minimizes the neutral current and satisfies the UBF constraint. However, the relationship between γ_b and γ_c and the magnitude of neutral current is not easy to obtain in real time, therefore a simpler approach to setting γ_b and γ_c is required. Instead, here we will consider γ_b and γ_c to be constrained to have a linear relationship given by:

$$|\gamma_b| + |\gamma_c| \leq \gamma_{max} \tag{21}$$

Where γ_{max} is the smaller of the intercepts of (20) on the γ_b, γ_c axes which is easily obtained as:

$$\gamma_{max} = min\left(\frac{0.02^2 - d}{a}, \frac{0.02^2 - d}{b}\right) \tag{22}$$

For ρ_b, ρ_c with the limits of [1, 0.98], γ_{max} has a small variation within the limits of [3.334°, 3.438°].

In summary, as shown in Fig. 4, the determination of the phase shift required to minimize neutral current can follow two steps. In the first step the phase shift angle required to give zero neutral current are calculated from (4), If these phase shifting angles calculated from (4) are within the phase shift constraint area, then they can be used directly as the reference phase shifting angle.

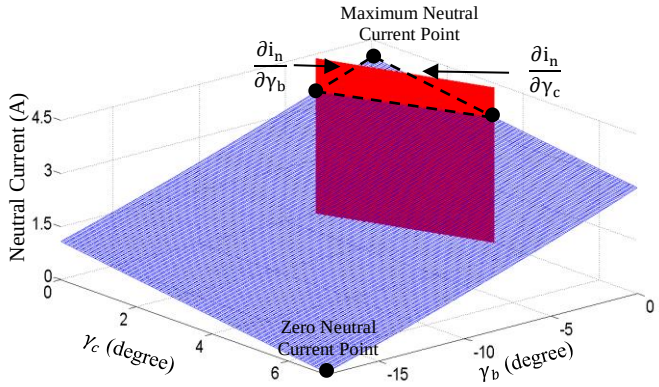

Fig. 4. The general relationship between phase shifting angle and neutral current with phase shift constraint

However if the phase shifting angle calculated from (4) violates the constraints, in order to find out the reference phase shift for the minimum neutral current, look for which derivative $\frac{\partial i_n}{\partial \gamma_b}$ or $\frac{\partial i_n}{\partial \gamma_c}$ is the larger and then set this phase shift at its maximum value, and the another equal to 0 as is indicated in Fig. 4. The maximum value for the phase shift angle is 3.24° as shown in (22).

Fig. 5 summarizes the detail of the method used for the neutral current minimization control. The voltage amplitude control section provides the amplitude of the reference voltage and also maintains the amplitude unbalance constraints. The amplitudes of the voltages are regulated to make the amplitudes of the resulting currents meet the constraints as obtained in phase shift control: $I_a \le I_b + I_c$, $I_b \le I_a + I_c$, $I_c \le I_b + I_a$. After the phase currents meet the phase current amplitude constraints, the phase shifting control section provides the phase angle reference, where the phase shifts are chosen as described above to either eliminate or minimize neutral current while also satisfying the phase unbalance degree constraints.

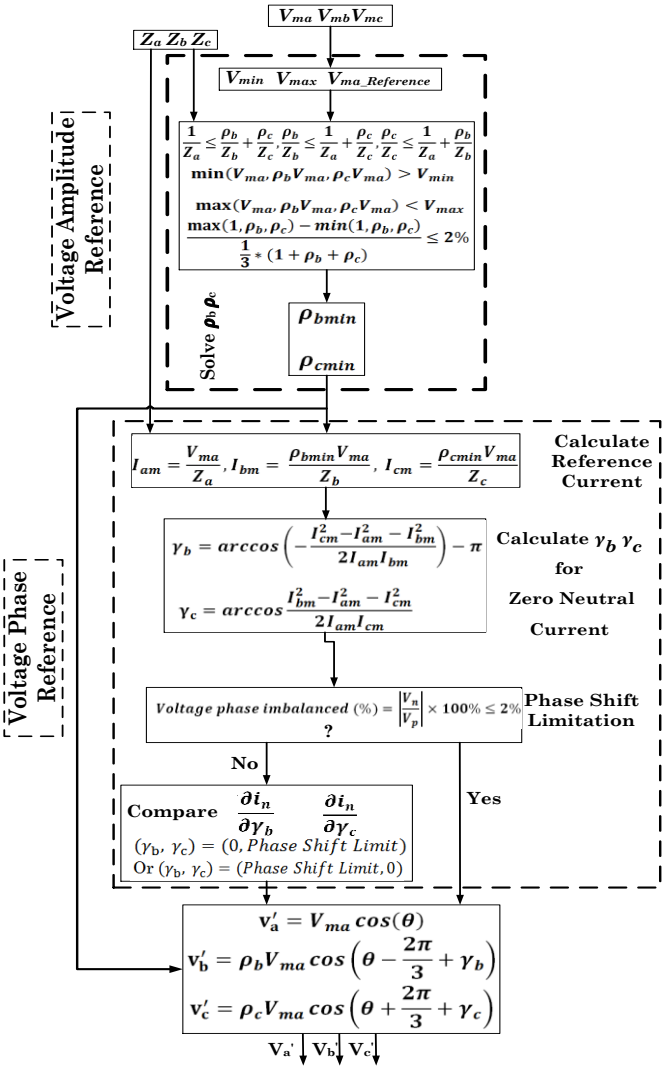

Fig. 5. The neutral current minimization control with references voltage.

V. Hardware Validation

In order to verify the control approaches described above, a 220 V, 2 kVA downscaled prototype of a three-phase four-leg inverter has been implemented with the hardware in the loop real time simulation platform from Opal-RT as shown in Fig.6. In this case the control algorithms and PWM are implemented in the OP5600 Series OPAL-RT simulators which are generated from the Matlab/Simulink models. The OP5600 Series OPAL-RT simulator also generates the firing pulses for the 4-leg inverter bridge which is based on the 8857-1 IGBT Chopper/Inverter from Lab-volt. As the key stage for dealing with the unbalanced load for SST is the output stage, for the sake of simplicity, only the inverter stage of the SST is implemented in the experiment. The tests compare results from two control methods, neutral current elimination control, and neutral current minimization control with limitations according to the EN 50160 unbalance standard. The parameters in Table. I are fixed for all of these tests. The recorded waveforms are inverter neutral current i_n, and output phase voltage v_a, v_b, v_c.

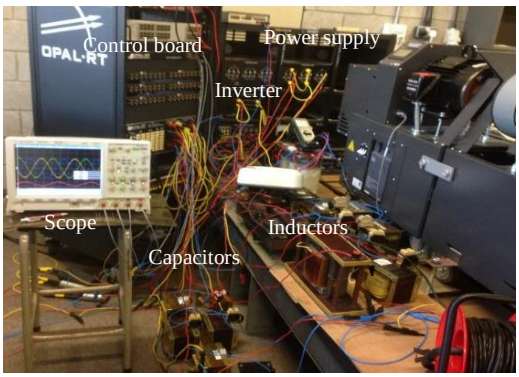

Fig. 6. Downscaled prototype of a three-phase four-leg inverter.

TABLE I
Simulation Parameters

Rated Power	2 kVA	**DC Bus Voltage**	440 V
Load Resistors	20/39/98 Ω	**Output Voltage**	220 V
Switching Frequency	3 kHz	**LC Filter**	80μF,65mH

A. Neutral Current Elimination Control

For neutral current elimination control, the output voltage has a larger variation on its amplitude than its phase angle as shown in the Fig. 7 (a). Because there was no limitation set for the voltage amplitude adjustment, the voltage amplitude regulation part in the control will adjust the amplitude of output voltage limited only by the phase current constraint. However, the phase shifting part regulates the phase angle to achieve the elimination of the neutral current. The result of elimination control is the almost total elimination of the neutral current after several cycles, although of course at the price of a very significant degree of unbalance in SST output voltage amplitude. Note the neutral current is not zero, because the experiment omits the correction for load angle.

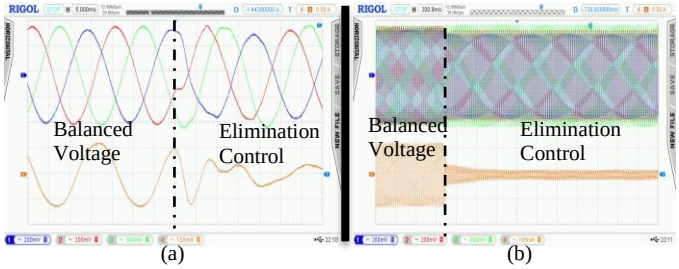

Fig. 7. Neutral current elimination control hardware test (a) variation point Part-graph; (b) stable performance. A: 48ohms+33 mH; B: 63ohms+33 mH; C: 98ohms+33 mH.

B. Neutral Current Minimization Control with Constraints

Fig.8 shows the test results for the application of the neutral current minimization where the output voltage unbalance in amplitude and phase is limited to be within the constraints set by the standard. Clearly the unbalance in the three phase output voltages is much less noticeable and the neutral current is successfully reduced, but not eliminated. Fig. 8 (a) shows a close up of the voltage at the instant of minimization control activation. Unlike neutral current elimination control, which requires time to coordinate the amplitude and phase, the neutral current minimization control can stabilize within one cycle. Fig. 8 (b) shows the longer time scale of the experiment with four sections. The load is balanced at the start with balanced voltage control, after which the load becomes unbalanced initially with balanced voltage control and then with the neutral current minimization control active, and finally returning back to balanced load at the end. This illustrates that the control not only succeeds in reducing the neutral current but also works on dynamic load variations. Table. II compares the results of SST with voltage balance, neutral current elimination and neutral current minimization control under one set of unbalanced loads.

TABLE II
Experiment Results Summary For Different Controls

Control Strategy	Neutral Current Amplitude (A)	Neutral Current Reduction (%)	Voltage Unbalance (%)
Balanced Voltage Control	2.1	0	0
Neutral Current Minimization	1.3	38%	1.5
Neutral Current Elimination	0.3	86%	62.3

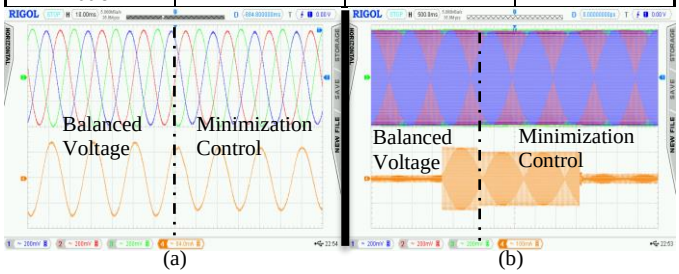

Fig. 8. Neutral current minimization control hardware test (a) variation point Part-graph, A: 48ohms+33 mH; B: 63ohms+33 mH; C: 98ohms+33 mH; (b) Complete graph, start from balanced load 25 ohms+33 mH, to unbalanced load A: 48ohms+33 mH; B: 63ohms+33 mH; C: 98ohms+33 mH, end to balanced load 25 ohms+33 mH.

Fig. 9 shows the neutral current minimization control under an asymmetric open fault test, where the load starts from a balanced load and subsequently has a single phase open fault as indicated by the sudden increase in neutral current. However in the face of the open fault, the control maintains the voltage balance thus validating that the proposed neutral current minimization can run stably in both normal operation and open faults.

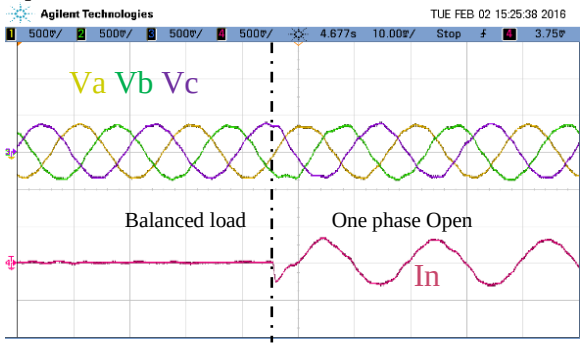

Fig. 9. Neutral current minimization control hardware test under open short, start from balanced load 25 ohms+33 mH, to phase A open.

VI. Performance in Distribution Network

Although the basic operation of the control has been validated in the previous section, it is now important to investigate the potential performance improvements obtained when the control is applied with degrees of load unbalance closer to those which occur in the distribution system. In order to validate and quantitatively compare the performance of these control strategies for more realistic degrees of load unbalance, simulation results are obtained for the unbalanced loading profile for a 400 kVA, 10 kV/400 V ENWL distribution network in the UK, consisting of 90 residential customers evenly distributed across three phases, as shown in Fig. 10 [33]. A winter day unbalanced three phase loading profile in each area with 1 minute time resolution based on the average yearly energy consumption is shown in Fig. 11 (left). The load is modelled as an exponential load with its voltage sensitivity set as indicated in Fig. 11 (right) [20][32].

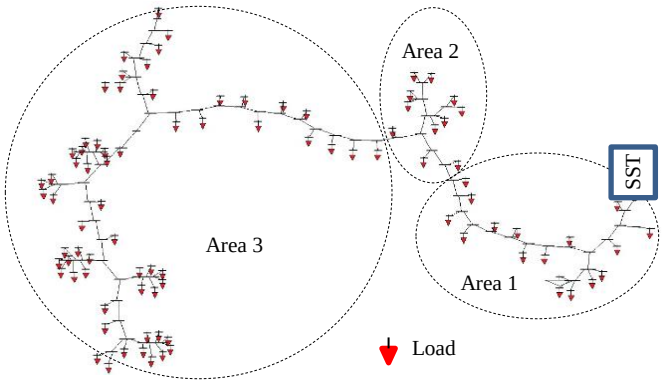

Fig. 10. Distributed loading network.

A. Network Dynamic Simulation

The network model is implemented in Matlab/Simulink, with a dynamic and continuously changing load. Fig. 11 shows the data for the total power consumption in each area, while the data for each customer is obtained by averaging the power in the corresponding phase and then randomizing between 90% to 110%. To speed up the simulation, the one

minute resolution in data is downscaled to 1 second in the simulation, i.e. 24 hour is represented by 1440 seconds. The SST is represented by a controllable voltage source with the balanced voltage control, neutral current elimination control and proposed neutral current minimization control.

Fig. 12 (a) shows the neutral current result at the SST terminal under the various controls. Clearly, compared with the balanced voltage control, the proposed neutral current minimization control reduces the neutral current, while the neutral current elimination control can eliminate the neutral current as expected. However, the latter one has a significant voltage unbalance degree in terms of both PVUR and UBF as shown in Fig. 12 (b) and (c) respectively. In particular it violates the PVUR standard all the time and peaks to approximately 115%. On the other hand the neutral current minimization control can maintain both PVUR and UBF below the 2% limit for the entire time.

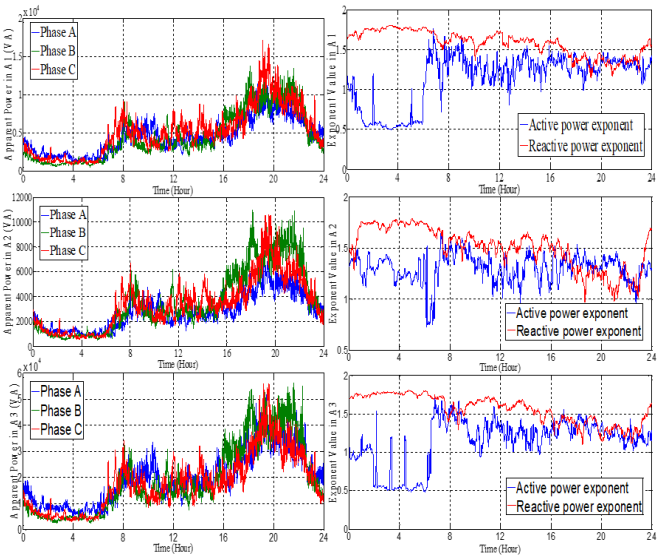

Fig. 11. Winter daily three phase loading profile in area 1, 2 and 3.

B. Network Static Simulation

The SST control algorithm regulates its output voltage in order to minimize the neutral current at the SST terminals although clearly this is not the same neutral current which will exist in all the other lines. Therefore, it is important to look at the effect of the neutral current minimization on the neutral current and losses in the other lines. The losses in the various sections of lines are calculated by determining the current and voltage for the various lines from the SST output voltage and the various loads in the different areas. The full network is too complex to present the neutral current in each line section, and therefore a simplified model with lines representing three areas as shown in Fig. 13 is used. The corresponding network data is given in the figure and the load data is the same as Fig. 11. Power flow analysis is performed using the Matlab fsolve function assuming static loads for each one minute of time resolution.

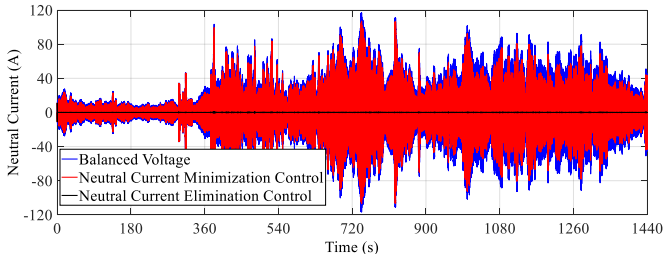

(a) Neutral Current

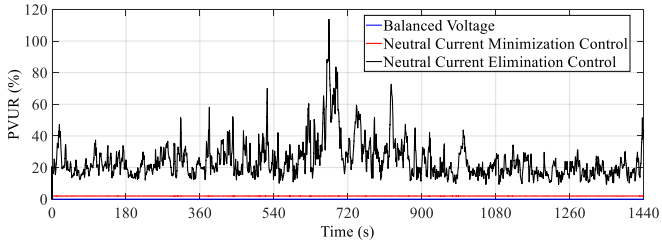

(b) Voltage Unbalanced Degree PVUR

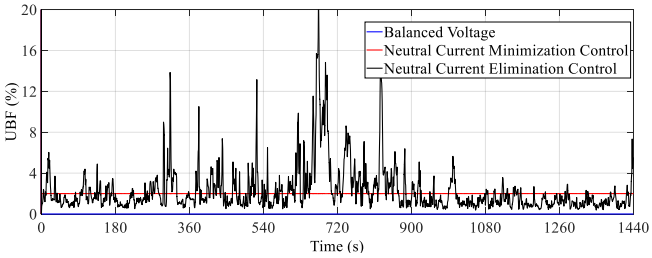

(c) Voltage Unbalanced Degree UBF

Fig 12. Distribution network Matlab/Simulink results.

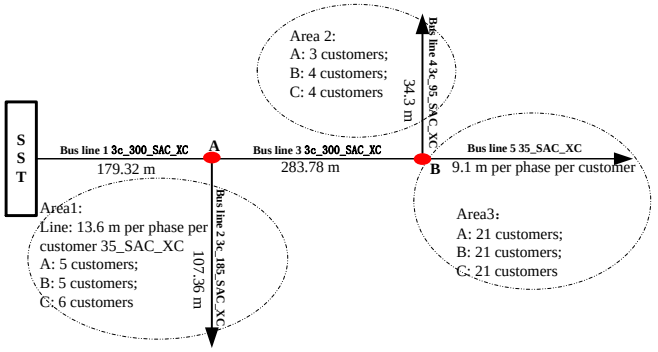

Fig. 13. Distributed loading network

The reduction in neutral current achieved by the neutral current minimization control as opposed to balanced voltage control for the above system specifications is shown in Fig. 14 for each of the lines. As expected, the neutral current minimization control can effectively reduce the neutral current in all lines although the reduction in some lines is more significant than others. As shown in Fig. 14 the minimization control can definitely reduce the neutral current in line 1 which is directly connected to the SST. The minimization control could also mainly reduce the neutral current on the lines which connect to the larger loads among the different areas, such as line 5 shown in Fig. 14 (Line 5). However, the minimization control may also increase the neutral current as shown in Fig. 14 Line 2 and 4. This is particularly the case in the areas with lower loading such as in area 2 which has only 9 customers. This is due to the fact that the unbalanced load degree in the small loading area is different from that in the

large loading area. Of course since the total neutral current is reduced, then if an increase occurs on some lines, this must be counteracted by a greater decrease on other lines.

The test results of total power energy consumption for balanced voltage and neutral current minimization control is summarized and compared in Table. III

In this situation, the neutral current minimization control not only reduces the loss from the cables but also the output load power. Compared with the energy saving from loss in the lines, considerably more energy is saved from the loading. This saving is attributed to the voltage amplitude adjustment aspect of the neutral current minimization control, which can decrease the voltage amplitude and hence reduce the power in the residential load

TABLE III
Daily Energy Consumption

Daily Energy	Balance Voltage Control	Neutral Current Minimization	Energy Saving
Output (kWh)	2027.8	1988	39.7 (1.96%)
Loading (kWh)	1978	1941	37.2 (1.88%)
Loss (kWh)	49.4	46.9	2.5 (5.06%)

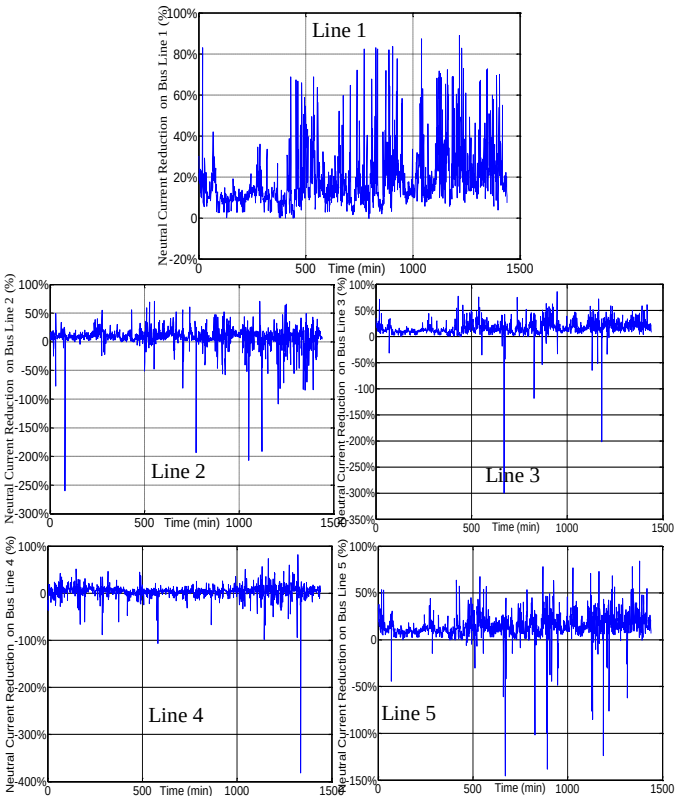

Fig. 14. Neutral current reduction with minimization control for the bus lines.

C. Control Comparison

Finally we compare the total neutral current and voltage unbalanced degree under the balanced voltage, neutral current elimination and neutral current minimization control. The graphs in Fig. 15 and Fig. 16 plot the neutral current in Line 1 and output voltage unbalance degree vs. the load unbalance degree, under the three control strategies.. It needs to be noted that the erratic nature of the curves in these graphs is due to the following reasons. As can be seen from Fig. 11, the jumps are obviously from the load changes with 1 minute time resolution. For Fig. 15, where the neutral current is plotted vs. load unbalance degree, it should be noted that similar load unbalance degrees may occur for very different loading levels and hence result in very different neutral currents. The results indicate that under the load unbalance conditions the elimination control can reduce the neutral current to approximately zero. However, in order to achieve this Fig. 16 shows that the required output voltage unbalance degree significantly exceeds the EN 50160 standard limitation when the load unbalance degree exceeds approximately 7%. In contrast, using both balanced output and the neutral current minimization control, the output voltage unbalance degree of the SST can maintain a value lower than the EN 50160 standard limitation with the variable loading unbalance degree. Of course the neutral current cannot be eliminated while adhering to these constraints, however use of the neutral current minimization control does result in a significantly reduced neutral current compared to the balanced output voltage situation.

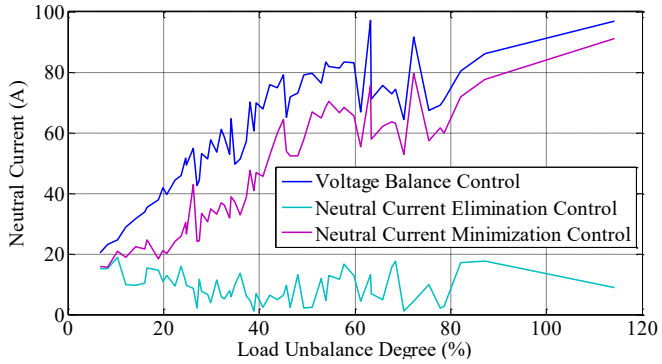

Fig. 15. Load unbalance degree vs neutral current (rms value).

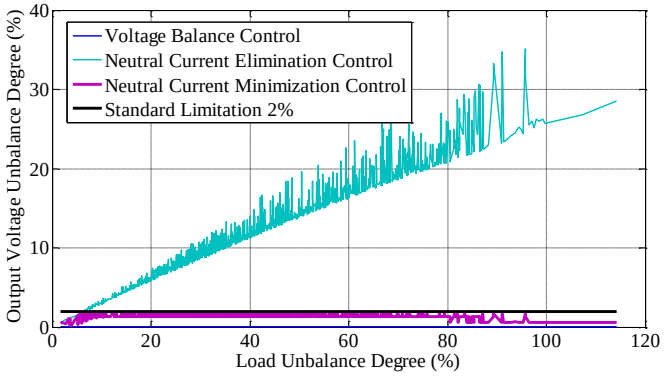

Fig. 16. Loading unbalance degree vs output voltage unbalance degree.

VII. Conclusions

Three control strategies have been evaluated for the SST output voltage which can eliminate the neutral current. The most effective of these is the combination control which works by making adjustment to both voltage amplitude and phase in order to eliminate neutral current. However, these techniques are not practical in reality because the level of load unbalance present in the distribution network is such that very large unbalance in the SST output voltage and phase would be required in order to totally eliminate the neutral current.

Therefore, a neutral current minimization control technique

had been developed which minimizes neutral current but still ensures that SST output voltage magnitude and phase unbalance are within the constraints imposed by the EN 50160 standard. The operation of the control has been validated by hardware tests. It has been shown that under the typical range of load unbalance seen in the distribution network this control approach can both reduce neutral current and ensure adherence to the standards.

The neutral current minimization control has then been applied to a model of a distribution network with distributed loads and a time varying daily loading profile. The results of this analysis have shown that although neutral current will not be minimized in all parts of the network, overall the neutral current minimization results in an energy saving from both reduced losses in the distribution cables and reduced power consumption in the load. The reduction in cable loss was shown to be of the order of 5.1%. The reduction of load power consumption was shown to be of the order of 1.9%. Therefore, the SST with the neutral current minimization control can potentially give significant energy savings in the distribution network.

VIII. References

[1] E. Ronan, S. Sudhoff, S. Glover, and D. Galloway, “A power electronic based distribution transformer,” *IEEE Trans. Power Delivery*, vol. 17, no. 2, pp. 537–543, Apr. 2002.

[2] X. She, A. Q. Huang and R. Burgos, "Review of Solid-State Transformer Technologies and Their Application in Power Distribution Systems," *IEEE J. Sel. Emerging and Selected Topics in Power Electronics*, vol. 1, no. 3, pp.186-198, Sept. 2013.

[3] A. Q. Huang, M. L. Crow, G. T. Heydt, J. P. Zheng, and S. J. Dale, “The future renewable electric energy delivery and management (FREEDM) system: The energy internet,” *Proc. IEEE*, vol. 99, no. 1, pp. 133–148, Jan. 2011.

[4] R. Zhu, G. De Carne, F. Deng and M. Liserre, "Integration of Large Photovoltaic and Wind System by Means of Smart Transformer," *IEEE Transactions on Industrial Electronics*, vol. 64, no. 11, pp. 8928-8938, Nov. 2017.

[5] X. Gao, F. Sossan, K. Christakou, M. Paolone and M. Liserre, "Concurrent Voltage Control and Dispatch of Active Distribution Networks by Means of Smart Transformer and Storage," *IEEE Transactions on Industrial Electronics*, vol. 65, no. 8, pp. 6657-6666, Aug. 2018.

[6] C. Kumar, R. Zhu, G. Buticchi and M. Liserre, "Sizing and SOC Management of a Smart-Transformer-Based Energy Storage System," *IEEE Transactions on Industrial Electronics*, vol. 65, no. 8, pp. 6709-6718, Aug. 2018.

[7] X. She, X. Yu, F. Wang and A. Q. Huang, "Design and Demonstration of a 3.6-kV–120-V/10-kVA Solid-State Transformer for Smart Grid Application," *IEEE Trans. Power Electron*., vol. 29, no. 8, pp.3982-3996, Aug. 2014.

[8] S. Madhusoodhanan et al.,”Solid State Transformer and MV Grid Tie applications enabled by 15 kV SiC IGBTs and 10 kV SiC MOSFETs based Multilevel Converters,” *IEEE Transactions on Industry Applications*, Vol.51, No. 4, July-Aug, 2015, pp3343-3360.

[9] L. Ferreira Costa, G. De Carne, G. Buticchi and M. Liserre, "The Smart Transformer: A solid-state transformer tailored to provide ancillary services to the distribution grid," *IEEE Power Electronics Magazine*, vol. 4, no. 2, pp. 56-67, June 2017.

[10] D. Shah and M. L. Crow, "Online Volt-Var Control for Distribution Systems With Solid State Transformers," *IEEE Trans. Power Del*, vol. 31, no. 1, pp 343 – 350, Feb. 2016.

[11] X. She, A. Q. Huang, S. Lukic and M. E. Baran, "On Integration of Solid-State Transformer With Zonal DC Microgrid," *IEEE Transactions on Smart Grid*, vol. 3, no. 2, pp. 975-985, June 2012.

[12] X. Yu, X. She, X. Zhou and A. Q. Huang, "Power Management for DC Microgrid Enabled by Solid-State Transformer," *IEEE Transactions on Smart Grid*, vol. 5, no. 2, pp. 954-965, March 2014.

[13] Q. Ye, R. Mo and H. Li, "Multiple Resonances Mitigation of Paralleled Inverters in a Solid-State Transformer (SST) Enabled ac Microgrid," *IEEE Transactions on Smart Grid*, 14 Feb. 2017.

[14] T. L. Vandoorn, J. D. M. De Kooning, B. Meersman, J. M. Guerrero and L. Vandevelde, "Voltage-Based Control of a Smart Transformer in a Microgrid," *IEEE Transactions on Industrial Electronics*, vol. 60, no. 4, pp. 1291-1305, April 2013.

[15] Z. X. Zou, G. Buticchi, and M. Liserre, “Analysis and stabilization of a smart transformer-fed grid,” *IEEE Transactions on Industrial Electronics*, vol. 65, no. 2, pp. 1325–1335, Feb 2018.

[16] Z. Zou, G. Buticchi and M. Liserre, "Grid Identification and Adaptive Voltage Control in a Smart Transformer-fed Grid," *IEEE Transactions on Power Electronics*. 13 June 2018.

[17] G. D. Carne, M. Liserre, and C. Vournas, “On-line load sensitivity identification in lv distribution grids,” *IEEE Transactions on Power Systems*, vol. 32, no. 2, pp. 1570–1571, March 2017.

[18] Z. X. Zou, G. D. Carne, G. Buticchi, and M. Liserre, “Smart transformer fed variable frequency distribution grid,” *IEEE Transactions on Industrial Electronics*, vol. 65, no. 1, pp. 749–759, Jan 2018.

[19] G. D. Carne, G. Buticchi, Z. X. Zou, and M. Liserre, “Reverse power flow control in an ST-fed distribution grid,” *IEEE Transactions on Smart Grid*, vol. PP, no. 99, pp. 1–1, 2017.

[20] J Chen, C O'Loughlin and T O'Donnell, “Dynamic demand minimization using a smart transformer,” Proc. 43rd Annual Conference of the IEEE Industrial Electronics Society, IECON 2017, Beijing, China, Dec. 2017, pp 4253 – 4259.

[21] P. Richardson, D. Flynn, A. Keane, “Impact assessment of varying penetrations of electric vehicles on low voltage distribution systems,” Proc. IEEE Power and Energy Soc. General Meeting, 2010, pp. 1 – 6

[22] A. von Jouanne, B. Banerjee, “Assessment of Voltage Unbalance,” *IEEE Transactions on Power Delivery*, vol. 16, no. 4, Oct. 2001.

[23] B. Singh, P. Jayaprakash, T. R. Somayajul, and D. P. Kothari, “Reduced rating VSC with a zig-zag transformer for current compensation in a three-phase four-wire distribution system,” *IEEE Trans. Power Del*., vol. 24, no. 1, pp. 249-259, Jan. 2009.

[24] R. M. Ciric, L. F. Ochoa, A. Padilla-Feltrin, and H. Nouri, “Foult analysis in four-wire distribtuion networks,” *Proc. Inst. Elect. Eng., Gen., Transm. Distrib*., vol. 152, no. 6, pp. 977-982, 2005.

[25] Z.-Q. Guo, I. V. Prasanna and S. K. Panda, “Design of New Control Strategies for a Four Leg Three-Phase Inverter to Minimize the Neutral Current Under Unbalanced Loads,” International Power Electronics Conference, Japan, 2014.

[26] S. Dasgupta, 1. V. Prasanna, S. K. Sahoo and S. K. Panda, “A novel four-leg three-phase inverter control strategy to reduce the Data Center thermal losses: Elimination of neutral current,” 38th Annual Conference on IEEE Industrial Electronics Society (IECON 2012), Montreal, QC, Canada, 25-28 Oct. 2012.

[27] H. Markiewicz and A. Klajn, “Power Quality Application Guide: Voltage Disturbances Standard EN 50160- Voltage Characteristics in Public Distribution Systems,” Copper Development Association IEE Endorsed Provider, July 2004,.

[28] S.Falcones, X.L.Mao, and R.Ayyanar, “Topology comparison for solid state transformer implementation,” in Proc.IEEE PES general meeting 2010, pp 1-8.

[29] T. Yang, R. Meere, C. O'Loughlin and T. O'Donnell, “Performance of solid state transformers under unbalanced loads in distribution systems,” In2016 IEEE Applied Power Electronics Conference and Exposition (APEC) 2016 Mar 20 (pp. 2629-2636). IEEE.

[30] R. Zhang, V. H. Prasad, D. Boroyevich, and F. C. Lee, “Three-dimensional space vector modulation for four-leg voltage-source converters,” *IEEE Trans. Power Electron*., vol. 17, no. 3, pp. 314–326, May 2002.

[31] P. Pillay and M. Manyage, “Definitions of Voltage Unbalance,” *Power Engineering Letters*, IEEE Power Engineering Review, May 2001.

[32] Electric Power Research Institute (EPRI) Report, “Measurement-Based Load Modeling,” Sep. 2006.

[33] K. McKenna and A. Keane, “Discrete Elastic Residential Load Response under Variable Pricing Schemes,” Innovative Smart Grid Technologies Europe (ISGT EUROPE), 2014 5th IEEE/PES, 12-15 Oct. 2014.

Junru Chen (S'17) received his ME Electrical Energy Engineering from University College Dublin in 2016. Since September 2016, he is a PhD student candidate with University College Dublin. His scholarship is funded through the SFI Investigator Award with title "Energy Systems Integration Partnership Programme". His current research interests in power electronics control, modelling, stability and application.

Tao Yang was born in Hunan, China, in 1987. He received the B.Eng. degree in electrical engineering from the Guangxi Teachers Education University, China, in 2009, the M.S. education in electrical engineering from the Guangxi University in 2009-2012 and the Ph.D. degree in electrical engineering with emphasis on power electronics from the University College Dublin, Dublin, Ireland in 2016; Since 2016, he has been with several high-tech companies including BYD¡¢SITECH etc. He is currently with WANMA GROUP, China, where he is the director of research Institute and is engaged in research and development on the electrical car charging devices and charging networking systems applications. His current research interests include electrical car charging devices¡¢high-power high-efficiency converter topologies, high-power-factor rectifiers, electric vehicles, and sustainable and renewable energy sources.

Cathal O'Loughlin was born in Dublin in 1968. He received a B.E. Degree in electrical engineering from University College, Dublin in 1990, and the MEngSc Degree in 1993. He joined Merrimack Transformers Ireland in 1993 as a design engineer where he remained until 2003. He was awarded Techstart Employee of the year 1994. After a period in non-engineering work he returned in 2010 as a researcher in a project to design, build and test a linear switched reluctance generator at the Institute of Technology, Blanchardstown, Dublin for 2 years. He then worked in Wavebob, a company involved with wave energy devices as a design engineer for a short period and then lectured Mathematics for 1 year in the Institute of Technology, Carlow (2012-2013). He has since been as a research Engineer in the Energy Institute, UCD. His research interests are electrical machines, power electronics and real time implementation.

Terence O'Donnell (M' 1995) is an associate professor in the School of Electrical and Electronic Engineering in University College Dublin. He is a principle investigator within the UCD Energy Institute where his research interests are focused on the use of power electronics converters in power systems and in particular on the interfacing of power electronics to the grid. Specifc interests include the grid applications of solid state transformers, the control of converters for distributed energy resources and the use of power hardware in the loop testing methods.

Terence has previously worked in the Tyndall National Institute in Cork where he has worked on numerous research projects, both at national and international level, relating to design, modelling and fabrication of magnetics for power conversion, magnetic field sensors, inductive powering and energy harvesting. Terence is an author on over 50 publications in peer reviewed journals.